

## Testing and Data Reduction of the Chinese Small Telescope Array (CSTAR ) for Dome A, Antarctica

Xu ZHOU<sup>1,4</sup>, Zhenyu WU<sup>1</sup>, Zhaoji JIANG<sup>1,4</sup>, Xiangqun CUI<sup>2,4</sup>, Longlong FENG<sup>3,4</sup>, Xuefei Gong<sup>2,4</sup>, Jingyao HU<sup>1,4</sup>, Qisheng LI<sup>1</sup>, Genrong LIU<sup>2</sup>, Jun MA<sup>1</sup>, Jiali WANG<sup>1,4</sup>, Lifan WANG<sup>3,4</sup>, Jianghua WU<sup>1</sup>, Lirong XIA<sup>2</sup>, Jun YAN<sup>1,4</sup>, Xiangyan YUAN<sup>2,4</sup>, Fengxiang ZHAI<sup>2</sup>, Ru ZHANG<sup>2</sup>, Zhenxi ZHU<sup>3,4</sup>

<sup>1</sup> National Astronomical Observatories, Chinese Academy of Sciences, Beijing 100012, China; [zhouxu@bao.ac.cn](mailto:zhouxu@bao.ac.cn)

<sup>2</sup> National Astronomical Observatories/Nanjing Institute of Astronomical Optics & Technology

<sup>3</sup> Purple Mountain Observatory

<sup>4</sup> Chinese Center for Antarctic Astronomy

Received [year] [month] [day]; accepted [year] [month] [day]

**Abstract** The Chinese Small Telescope ARray (hereinafter CSTAR) is the first Chinese astronomical instrument on the Antarctic ice cap. The low temperature and low pressure testing of the data acquisition system was carried out in a laboratory refrigerator and on the 4500m Pamirs high plateau, respectively. The results from the final four nights of test observations demonstrated that CSTAR was ready for operation at Dome A, Antarctica. In this paper we present a description of CSTAR and the performance derived from the test observations.

**Key words:** instrumentation: detectors — techniques: photometric — stars: variables

### 1 INTRODUCTION

Site testing at the South Pole (90°south, 2835 m elevation) and Dome C (123°east, 75°south, 3260 m elevation) over the past decade has shown that the Antarctic plateau offers outstanding sites for astronomical observations. The extremely cold temperatures lead to very low infrared backgrounds and atmospheric water vapor content. The very low wind speeds and stable middle and upper atmosphere result in favorable seeing conditions for high-resolution imaging (Storey et al. 2007). The median free-atmosphere seeing in Dome C is 0.27 arcsec, and it is below 0.15 arcsec for 25 per cent of the time (Lawrence et al.2004). In addition, the long dark winter on the Antarctic plateau allows continuous observations of variable astronomical objects.

Dome A (77°21'east, 80°22'south, 4093 m elevation), the highest point on the Antarctic plateau, is widely predicted to be an even better astronomical site even than Dome C, based on the topographic similarity and Dome A's higher altitude. In January 2005, via overland traverse, Dome A was first visited by the Polar Research Institute of China (hereinafter PRIC). This provides astronomers with a good opportunity to explore this special area for astronomy. PRIC plans to establish a permanently manned station at Dome A within the next decade, with astronomy as one of the scientific goals of the station. As part of this program, PRIC conducted a second expedition to Dome A, arriving via overland traverse in January 2008. On this expedition, the first Chinese Antarctic astronomical instrument, CSTAR, was deployed to Dome A. Beside the task of the astronomical site testing, the main scientific goals of CSTAR

include variable star light curves and statistics, supernovae studies, gamma-ray burst optical afterglow detection and exoplanet detection.

CSTAR was designed and constructed during 2006 – 2007 at the National Astronomical Observatories of China (NAOC) and the Nanjing Institute of Astronomical Optics Technology of China (NIAOT). A series of tests were performed on CSTAR before the second expedition to Dome A to ensure that it was ready for deployment. As a result of this careful preparation, CSTAR operated successfully during 2008, as part of the Plateau Observatory (PLATO) at Dome A (Yang et al. 2009). In Section 2, we describe the design and construction of CSTAR. Test observations at the Xinglong station of NAOC and the data reduction are presented in Section 3. Finally, a summary is given in Section 4.

## 2 INSTRUMENTS

CSTAR is a small  $2 \times 2$  Schmidt-Cassegrain telescope array. Each telescope of CSTAR has an entrance pupil diameter of 145 mm (effective aperture of 100 mm) and a focal ratio of  $f/1.2$ , giving a field of view of  $\sim 4.5^\circ \times 4.5^\circ$ . Fig. 1 shows the optical design of the CSTAR telescope, which consists of a catadioptric objective with spherical primary mirror, delivering low chromatic aberration. The first plano lens serves both as a window and as a filter. In order to keep the focus unchanged through a  $\sim 100^\circ\text{C}$  temperature difference (from 20 to  $-80^\circ\text{C}$ ), Zerodur and fused silica are used for the main optical components and Invar 36 is used for the telescope tube. The tube is designed to be light weight, well sealed, and easy to assemble. The inside of the telescope tube was filled by pure nitrogen to avoid ice and frost formation on the internal optical surfaces. Each telescope tube is hermetically sealed and an ITO (Indium-Tin-Oxide) film was coated onto the front window. An electric current is passed through this film, providing  $\sim 10$  W of power to keep the surface of the window warmer than ambient. CSTAR is specifically designed for Antarctic operation, having no moving parts at all—including the optics and mechanical supporting system. The four telescopes are installed in a steel enclosure, see Fig. 2, and are pointed at the South Celestial Pole; i.e., each telescope is inclined  $9^\circ 38'$  from the zenith. Details of the CSTAR telescope structure are described in Yuan et al. (2008).

The three telescopes CSTAR #2, #4, and #1 have fixed filters:  $g$ ,  $r$ , and  $i$ , the fourth telescope CSTAR #3 is filter-less. The main parameters of the three filters are listed in Table 1 and the transmission curves of those filters are presented in Fig. 3. The filters are designed to be similar to the corresponding filters of the SDSS (Fukugita et al. 1996). Using these filters, CSTAR can obtain multicolor photometric data for each object simultaneously.

An Andor DV435  $1\text{K} \times 1\text{K}$  frame transfer CCD with a pixel size of  $13 \mu\text{m}$  is used for the detector. Frame transfer technology is ideal for fast imaging as it has the advantage of requiring no mechanical shutter. Avoiding the need for moving parts is very desirable on the Antarctic plateau. The CCD was enclosed in a control box, as shown in Fig. 4. The cable at the back of the box connects to the PCI controller card installed in the control computer. The typical readout noise of the CCD is  $\sim 3 e$  with maximum of  $\sim 12 e$ , and the gain is set to  $2.0 e$  per A/D. The peak quantum efficiency of the Andor CCD at  $-90^\circ\text{C}$  is  $\sim 95\%$ . During the typical exposure time of 30 s and under the typical ambient temperatures of less than  $-50^\circ\text{C}$  on the Antarctic plateau, the dark current of the Andor CCD is only  $0.5 e$ . The dark current can thus be negligible under Antarctic conditions.

Each Andor CCD is controlled through the CCI-010 PCI controller card installed in an industrial control computer for each telescope. The control computer is composed of a 1TX-i7415VL main board, Intel Centrino 1.6 GHz CPU, and 1 GB of memory. Two kinds of storage disks are used for the control computer. One is a 4 GB CompactFlash (CF) disk which can operate at low temperatures (down to nearly  $-45^\circ\text{C}$ ); the other is a normal 750 GB IDE hard disk. Fig. 5 shows the four control computers. Each computer weighs 8.3 kg. The Windows operating system is installed onto the CF disk because of its greater reliability under low temperature conditions, while the 750 GB hard disk is mainly used as data storage. The CCD control and data collection software were developed based on the Andor-SDK-CCD software development kit for the Windows-XP operation system. The time of the controller computer of CSTAR #3 is synchronized by GPS and the other computer correct its clock by CSTAR #3.

The real time data reduction process start automatically after the controller computer booting. The image coorrected by bias and flat-field frames, and the catalogues objects is produced. The brightest 3000 stars of the catalogue from 1/3 images is moved to a special directory for data transfere via iridium satellite communication.

### 3 TESTING AND DATA REDUCTION

#### 3.1 Testing

In order to assure the performance of CSTAR under the extremely low temperature conditions of Dome A, the CCD system and several different industrial control computers were tested. Finally, the whole CSTAR system was tested at low temperature in the laboratory of NAOC. These tests indicated that the four telescopes and the CCD can work at low temperatures down to nearly  $-80^{\circ}\text{C}$ , while the four control computers can work down to  $-30^{\circ}\text{C}$ . In 2007 February 6 – 9, the CCD and control computers were tested at Kalasu. Kalasu (see Fig 4) is located in the Tajik Autonomous County of Taxkorgan, on the Xinjiang Pamirs of China at an elevation of 4450 m. We chose Kalasu as the test site because of its low temperature and low atmospheric pressure conditions similar to the Antarctic plateau. The atmospheric pressure was  $\sim 58.6$  kPa and the temperatures ranged from  $-5^{\circ}\text{C}$  to  $-18^{\circ}\text{C}$  during the testing process. Both the CCD and the control computers were shown to work normally during the two days of testing, and there are 4 750GB normal hard disks were selected as data storage of CSTAR.

In 2007 September 3 – 7, test observations of CSTAR were performed at the Xinglong station of NAOC. The four CCDs were cooled down to  $-40$  –  $-50^{\circ}\text{C}$  by electronic cooling system of the camera. The weather was good in most of the time during four observation nights, and more than 20,000 images were obtained. The typical exposure time was 20 s. Fig 6 shows the ‘super’ bias images for each telescope, which are the median of 100 bias frame images for each telescope. There is no obvious variation and structure in the ‘super’ bias images. These ‘super’ bias images are unique bias frames to be used for reduction of data both from observations at Xinglong and also from Dome A.

Variations of night-sky background are obvious even in the zenith direction. If one takes the time during a photometric, moonless night to obtain a long series of sky-dominated images pointing directly at the zenith, the effects of the nonuniformity of the night sky can be minimized. However, our telescope observes the polar sky area at an airmass of 1.54 at Xinglong station. The median sky background can only be used as an initial flat-field for image correction. Thus, we typically obtained ‘supersky’ flat-fields by combining images of the sky (Zhou et al. 2004). During this combination, the bright stars in the images were masked and rejected, and only the areas free from stars were used. By comparing the images, the median level of each pixel could be selected to derive the final ‘supersky’ flat-field. 100 images of ‘supersky’ for each telescope of CSTAR were used to obtain the ‘supersky’ flat-field. These flat-fields mostly reflect the small, pixel to pixel variations in the images. Fig. 7 shows the final ‘supersky’ flat-field images for each telescope. Some obvious structures can still be seen.

#### 3.2 Data reduction

First, for each filter a ‘super’ bias frame was subtracted from each image, then the ‘supersky’ flat-field was divided by the bias-corrected images. The bias and flat-field corrected data of  $\sim 20000$  images obtained by CSTAR during the four test-observation nights were processed with the automatic data reduction software developed by Z. J. JIANG and X. ZHOU based on the DAOPHOT photometric package (Stetson 1987), which was used in the data reduction of BATC (Fan et al. 1996; Wu et al. 2007). Because CSTAR has a large field and is undersampled, obtaining an accurate point-spread function (PSF) for the sources detected across the whole view of field is very difficult. The DAOFIND program was used to find stars in each image and DAOPHOT was used to perform synthetic aperture photometry on the objects detected by DAOFIND. All instrumental magnitudes of the four telescopes were then normalized to the  $V$  band magnitudes of stars in the image 39530013.fit, which was observed by #3 telescope on 2007 September 5.

### 3.3 Error analysis and correction

There are obvious systematic errors in the derived aperture-photometry magnitudes. The errors mainly come from following sources:

1. The bias stability of each CCD

Due to the continuous observation during exposures and the frame transfer mode of the CCD, there is no opportunity to obtain real-time bias frames. The bias frames obtained at one time must be used for observations from another day at Dome A. Because of variations in the environmental parameters, such as temperature and instrumental status, the bias of each CCD camera may change. This variable bias will introduce linear errors in the observed magnitudes.

2. Non-uniformity of the ‘supersky’ flat-field.

The flat-field images were not obtained during ideal photometric nights, and not from the zenith sky. A brightness gradient and asymmetry may exist in the flat-field frames. The variation in temperature from  $-40$  to  $-80^{\circ}\text{C}$  may also change the characteristics of the flat field. During the polar observations by the fixed CSTAR telescopes, every star will trace out a circle on the CCD, and the residual flat-field error will give a false variation in the observed magnitude of each star.

3. Variable PSF for stars in different positions in the images of CSTAR .

The telescopes of CSTAR have a large field of view. The optical design cannot keep the PSF exactly uniform over all parts of the image. When we use a fixed aperture to measure the magnitudes of the stars, the PSF depends on the location on the image and this will cause a variation in the instrumental magnitudes of each star relate to the other stars.

Because we are observing a single area of the sky, and the sky’s image is rotating on the CCD, we have the opportunity to correct the main residual system errors mentioned above. Using thousands of stars with very different magnitudes, we can easily determine the variable component of the bias residuals based on the different magnitudes of those stars in two different images. Using all of the circular traces of the stars, the large-scale residual flat-field correction can be obtained. Using the instrumental magnitudes from several different apertures for each star, the aperture photometry curve-of-growth can be obtained in all parts of the image but is mainly corrected with residual flat-field correction mentioned above. The instrumental magnitude obtained from different aperture were calibrated to the standard system. After all these corrections, the systematic errors in the derived photometric magnitudes can be reduced to the level of 0.01 mag for the brightest stars in most of the images. Some sudden abnormal variations, where they exist, mostly come from the cirrus clouds in the sky. Fig. 8 presents the magnitude-corrected flat-field images for each telescope using thousands of stars., and shows the obvious circular structures that match the traces of stars on the CCD.

Two kinds of error estimates have been performed. One is theoretic statistical estimation based on star’s magnitude and its sky background. The other is obtained by real repeated observation of all the objects in the images. By comparing the errors resulting from different images of the same field with the same filter, we find that the measurement errors are normally  $\pm 0.01$  mag for bright stars. The statistical errors can be regarded as the lower limits of the measurement errors. In the error estimates, we ignore points with abnormally large deviations to calculate the root mean square (rms) errors. The abnormal variation may come from the true star brightness variation, or defect of the image (cosmic ray, satellites, bad pixels, etc). Fig. 9 shows the photometric errors for each telescope of CSTAR at different magnitudes. Because the errors estimated by this method include real statistical errors and residual system errors from the bias and flat-field correction, the errors shown in Fig. 9 should be larger than the actual observational errors. Fig. 9 also shows that the efficiency of telescope #2 of CSTAR is very low and that the limiting magnitude of this telescope is about 2 mag lower than that of the other three telescopes. We knew that the CCD camera for CSTAR #2 was much noisier than the others, but we were unable to change it in the time available.

As an example of the data obtained, the light curve of one of the bright stars from the four CSTAR telescopes are shown in Fig. 11. The main scientific objectives of CSTAR are to assess the site quality of Dome A and to study the variable objects in the region of the South Pole. Fig. 10 shows the image

**Table 1** Passband parameters of filters used by CSTAR .

telescope	CSTAR #2	CSTAR #4	CSTAR #1	CSTAR #3
filter	<i>g</i>	<i>r</i>	<i>i</i>	none
effective Wavelength (nm)	470	630	780	
FWHM (nm)	140	140	160	

39530013.fit obtained by CSTAR during the test observations at the Xinglong station of NAOC. The variable stars detected by CSTAR are labeled by green circles. The light curves of those variable stars are presented in Fig. 12.

#### 4 CONCLUSIONS

CSTAR, China's first Antarctic astronomical instrument is described. CSTAR is composed of four small Schmidt-Cassegrain telescopes. Each telescope has an effective aperture of 100 mm and a field of view of  $\sim 4.5^\circ \times 4.5^\circ$ . Three of the four telescopes are equipped with *g*, *r*, *i* filters, the fourth one is filterless. A frame-transfer Andor DV435 1K $\times$ 1K CCD is used as the detector on each telescope. A specially designed control computer for each telescope is used for data acquisition and data reduction.

Low-temperature laboratory testing demonstrates that the telescopes and the CCD can work under extremely low temperature (down to nearly  $-80^\circ\text{C}$ ), while the control computer can work at temperatures as low as  $-30^\circ\text{C}$ . Actual test observations at Kalasu in the Xinjiang Pamirs indicated that the CCD and control computer can work at these low temperatures and under low atmospheric pressure conditions.

'Super' bias and 'supersky' flat-field images were obtained during the test observations at the Xinglong station of NAOC. These test observations and the subsequent data reduction indicate that CSTAR can work stably and obtain a large volume of scientific data. A special data reduction method was used to reduce the observational errors for each of the objects detected by CSTAR. The data reduction process is done automatically in real time, and catalogue of brightest star from 1/3 of the images obtained are prepared for further data transfer via iridium satellite communication. Finally, Eight variable stars were detected by CSTAR during the test observations.

**Acknowledgements** This work was supported by the Chinese National Natural Science Foundation grants No. 10873016, 10633020, 10603006, and 10803007, and by National Basic Research Program of China (973 Program), No. 2007CB815403. We thank our colleagues at the University of New South Wales, Australia, for assistance in editing this paper.

#### References

- Lawrence, J. S. Ashley, M. C., Tokovinin, A., & Travouillon, T. 2004, *Nature*, 431, 278  
 Fan, X.H., et al. 1996, *AJ*, 112, 628  
 Fukugita, M., et al. 1996, *AJ*, 111, 1748  
 Stetson, P.B. 1987, *PASP*, 99, 191  
 Storey, J. W. V., Lawrence, J. S., & Ashley, C. B. 2007, *RevMexAA*, 31, 25  
 Wu, Z. Y., et al. 2007, *AJ*, 133, 2061  
 Zhou, X., et al. 2004, *AJ*, 127, 3642  
 Yang, H.G., et al. 2009, *PASP*, 121, 174  
 Yuan, X.Y., et al. 2008, *SPIE*, 7012, 152

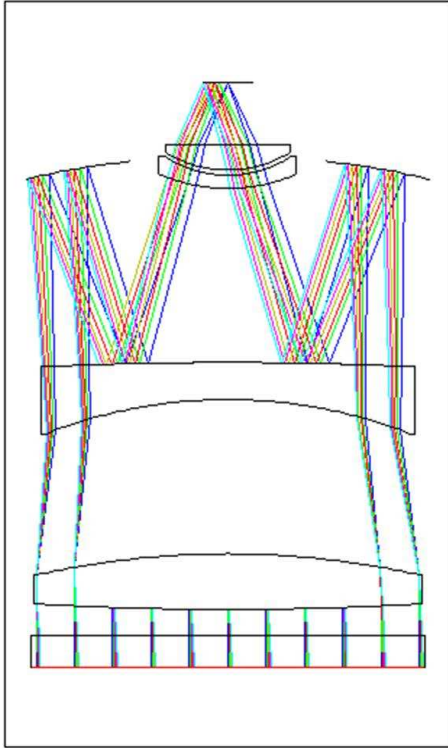


**Fig. 1** Optical design of CSTAR telescope.



**Fig. 2** A picture of CSTAR enclosure was taken in XingLong station of NAOC.

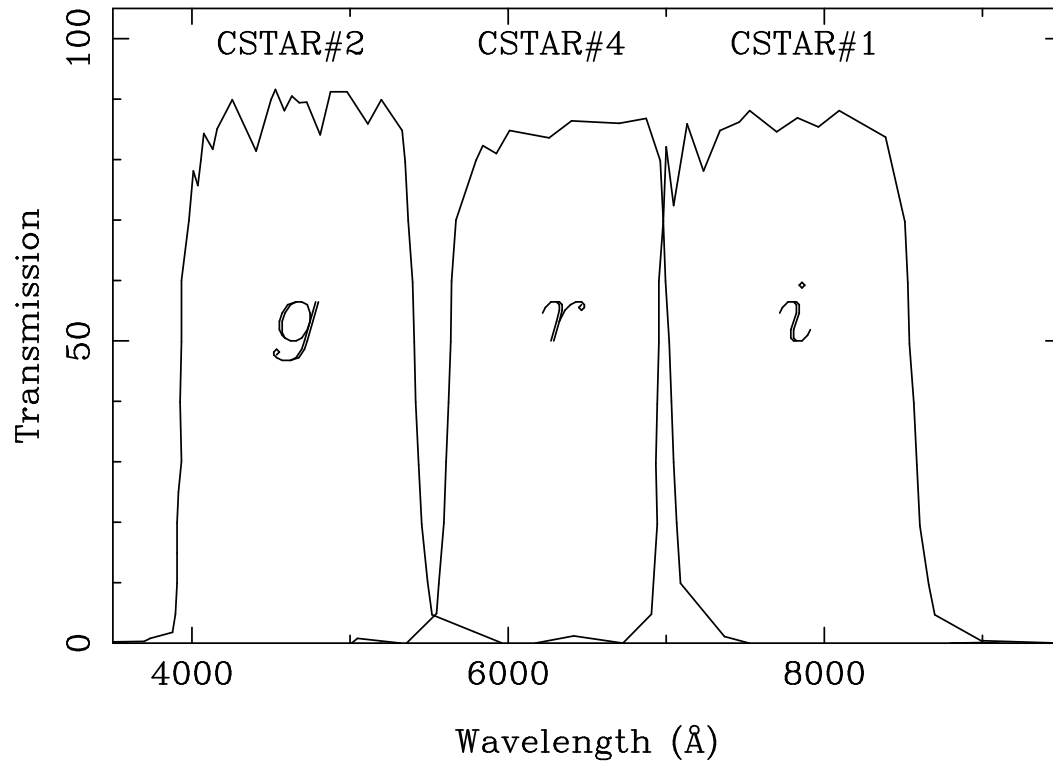


**Fig. 3** Transmission profiles of the 3 CSTAR filters. The filter codes (see Table 1) are labeled on each filter. Note that CSTAR #3 has no filter.





**Fig. 4** The Andor CCD enclosed in its control box. This picture was taken at Kalasu in the Tajik Autonomous County of Taxkorgan, Xinjiang Pamirs of China.



**Fig. 5** Computer control equipment.

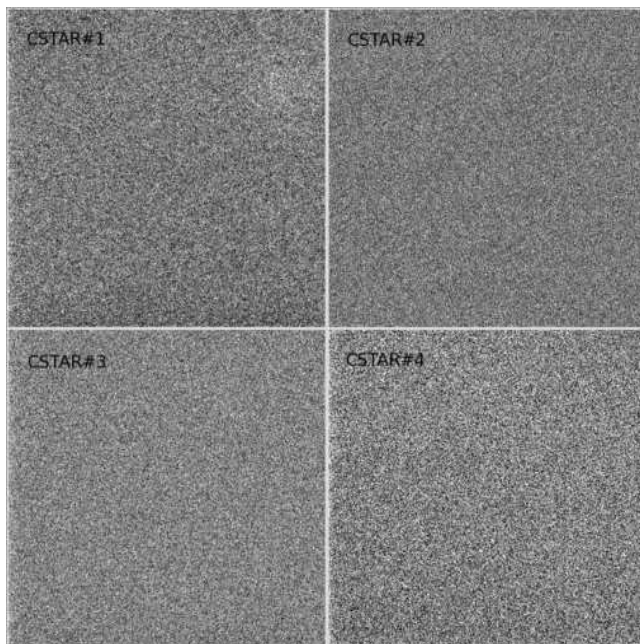


**Fig. 6** Bias frame images for each telescope.

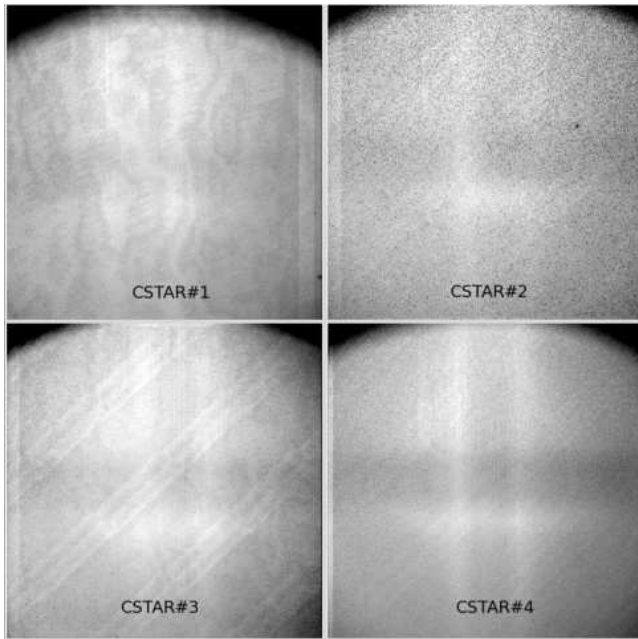


**Fig. 7** Flat-field images for each telescope.

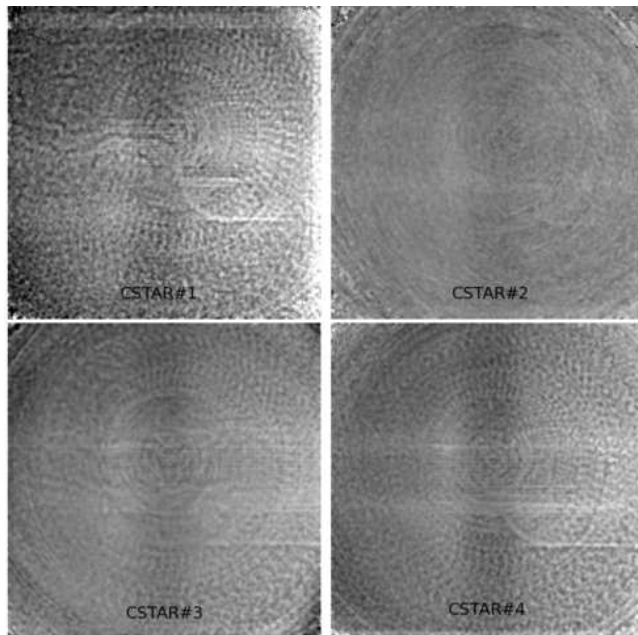


**Fig. 8** Images of the corrected flat field for each telescope.

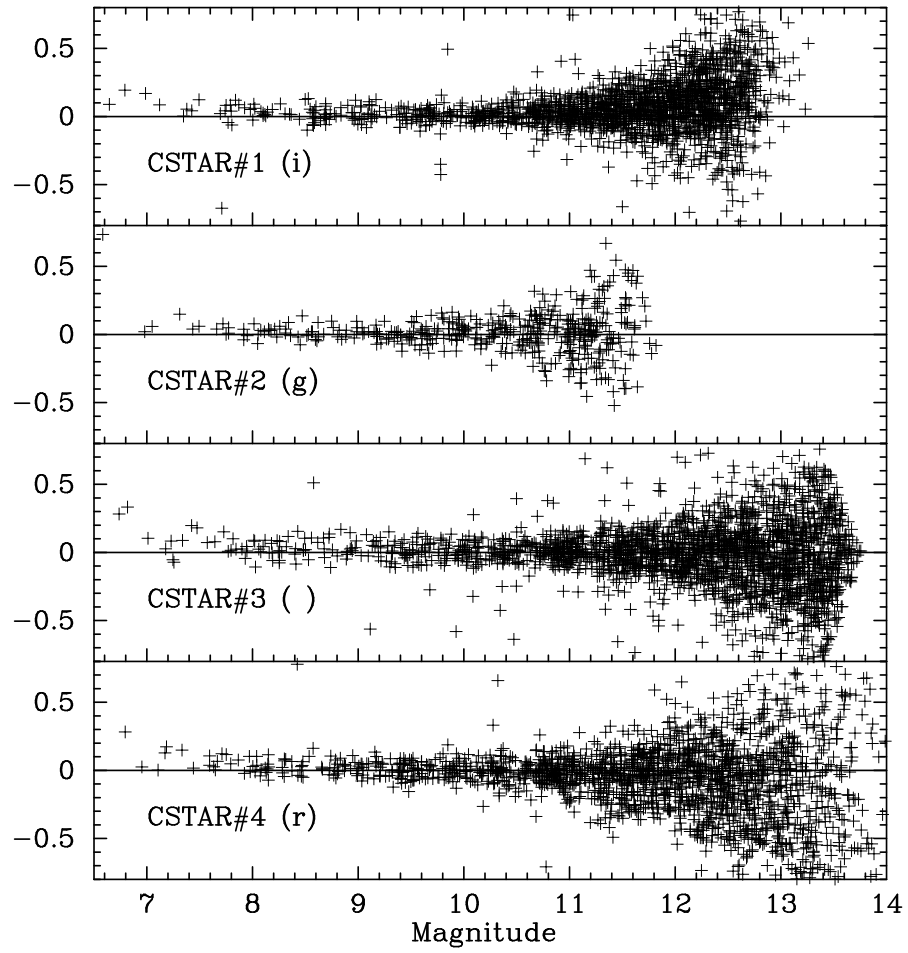


**Fig. 9** Photometric errors for each telescope of CSTAR . The vertical scale is in magnitudes.

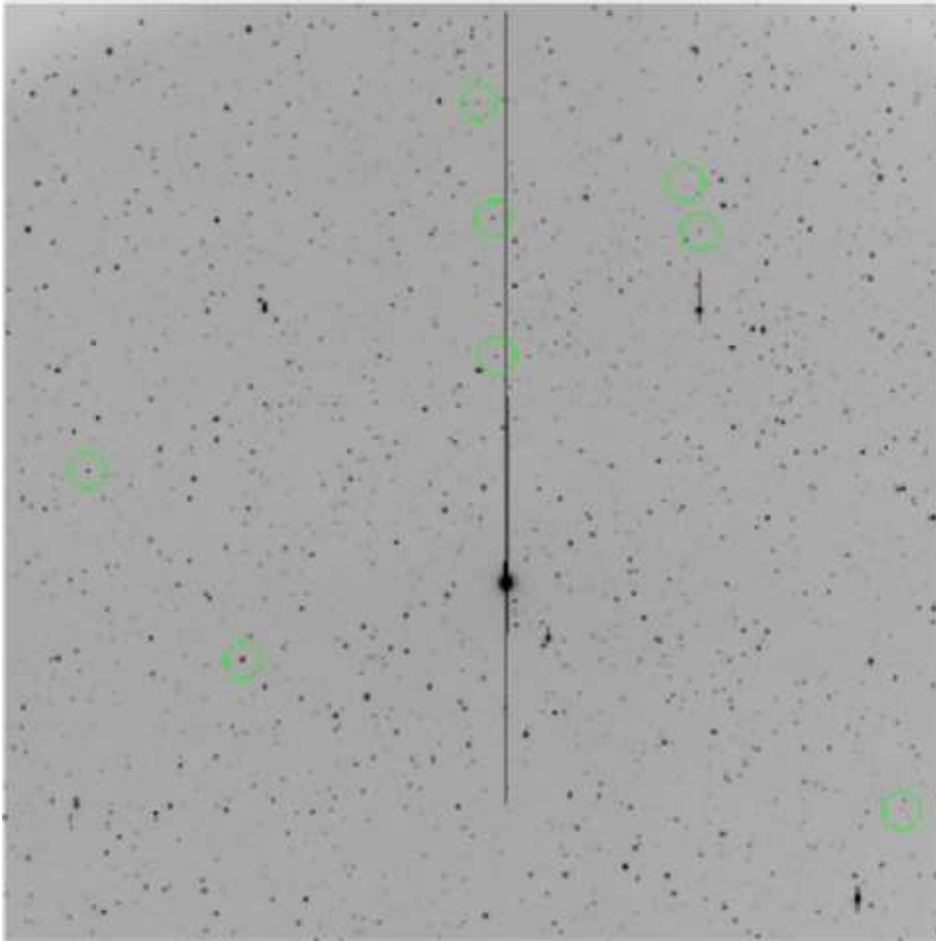


**Fig. 10** The image 39530013.fit obtained by CSTAR . The variable stars detected by CSTAR are labelled by green circles in the image.

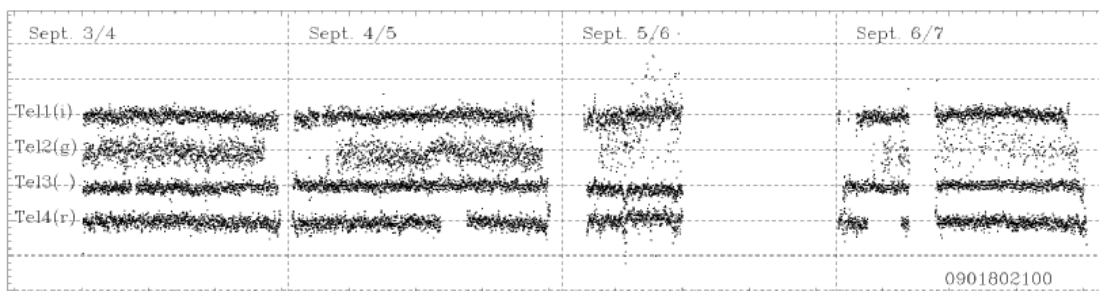


**Fig. 11** The light curve of one of the bright sources from the CSTAR telescopes.

